JOURNAL OF VIROLOGY, July 2007, p. 7716–7724 Vol. 81, No. 14
0022-538X/07/$08.00+0 doi:10.1128/JVI.00549-07

An RNA Stem-Loop within the Bovine Coronavirus nsp1 Coding Region Is a *cis*-Acting Element in Defective Interfering RNA Replication▽

Cary G. Brown,† Kimberley S. Nixon, Savithra D. Senanayake,‡ and David A. Brian*

Departments of Microbiology and Pathobiology, University of Tennessee College of Veterinary Medicine, Knoxville, Tennessee 37996-0845

Received 15 March 2007/Accepted 26 April 2007

Higher-order *cis*-acting RNA replication structures have been identified in the 3′- and 5′-terminal untranslated regions (UTRs) of a bovine coronavirus (BCoV) defective interfering (DI) RNA. The UTRs are identical to those in the viral genome, since the 2.2-kb DI RNA is composed of only the two ends of the genome fused between an internal site within the 738-nucleotide (nt) 5′-most coding region (the nsp1, or p28, coding region) and a site just 4 nt upstream of the 3′-most open reading frame (ORF) (the N gene). The joined ends of the viral genome in the DI RNA create a single continuous 1,635-nt ORF, 288 nt of which come from the 738-nt nsp1 coding region. Here, we have analyzed features of the 5′-terminal 288-nt portion of the nsp1 coding region within the continuous ORF that are required for DI RNA replication. We observed that (i) the 5′-terminal 186 nt of the nsp1 coding region are necessary and sufficient for DI RNA replication, (ii) two *Mfold*-predicted stem-loops within the 186-nt sequence, named SLV (nt 239 to 310) and SLVI (nt 311 to 340), are supported by RNase structure probing and by nucleotide covariation among closely related group 2 coronaviruses, and (iii) SLVI is a required higher-order structure for DI RNA replication based on mutation analyses. The function of SLV has not been evaluated. We conclude that SLVI within the BCoV nsp1 coding region is a higher-order *cis*-replication element for DI RNA and postulate that it functions similarly in the viral genome.

cis-acting RNA signaling elements that function directly in the replication of positive-strand viral genomes have been often first identified in helper virus-dependent defective or defective interfering (DI) RNAs (18, 26). One advantage in using DI RNAs for this identification is that *cis*-acting signals for replication can be evaluated independently from other functions for the same structure. Such functions might include encoding a *trans*-acting factor or regulating the synthesis of a *trans*-acting factor (e.g., regulation of translation to produce a replicase). With the use of a 2.2-kb DI RNA of the bovine coronavirus (BCoV), a molecule composed of only the two ends of the viral genome (8), primary and higher-order *cis*-replication structures have been identified in both the 3′ and 5′ untranslated regions (UTRs) (described below). Other *cis*-replication structures in these regions, identified first in the closely related mouse hepatitis coronavirus (MHV) genome, have also been found in the BCoV DI RNA (described below).

Three *cis*-replication elements have been identified in the 289-nucleotide (nt) BCoV 3′ UTR: (i) a bulged stem-loop beginning just downstream from the stop codon of the N gene (20, 21) and an adjacent pseudoknot (45), which possibly together act as a single higher-order molecular switch (14). The bulged stem-loop was first identified in the MHV genome (20–22). An important part of the switch concept derives from the existence of a 5-nt sequence that can function as a component of either the bulged stem-loop or the pseudoknot, but not both simultaneously (14). The bulged stem-loop–pseudoknot structure appears as a common feature among group 2 coronaviruses and has been analyzed in most detail in the context of the MHV genome (14). (ii) A complex bulged stem-loop near the 3′ terminus of the 3′ UTR, which contains the coronavirus common GGAAGAGC octamer sequence and an adjacent helical region (H. Y. Wu and D. A. Brian, unpublished). This structure was first identified in an MHV DI RNA (47). (iii) A 3′-terminal poly(A) tail (42; S. D. Senanayake and D. A. Brian, unpublished). Interestingly, to date only cellular proteins have been shown to interact with the 3′ UTR structures, and of these, only the 3′-terminal octamer-associated bulged stem-loop region (32, 47, 48) and the poly(A) tail (42) have been shown to be targets. The *cis*-acting functions of the 3′ UTR elements may be common among the group 2 coronaviruses, since the BCoV DI RNA can replicate with the helper function of several group 2 coronaviruses (46), and the entire 3′ UTR of the BCoV and of human severe acute respiratory syndrome-associated coronavirus (SARS-CoV) can functionally replace the 3′ UTR in the MHV genome (16, 21).

Three *cis*-replication elements have been identified in the 210-nt BCoV 5′ UTR. (i) The 5′-terminal 90-nt region harbors stem-loops SLI (nt 11 to 42) and SLII (nt 51 to 84) as predicted by the Tinoco algorithm and as supported by structure probing (8, 9). 5′-terminal deletions of up to 13 nt kill DI RNA replication (8), and other mutations made within the first 90 nt rapidly revert to the wild-type (wt) sequence (9) by a high-frequency recombination event with the helper virus genome, known as leader switching (28). Thus, it appears that the sequence and/or the stem-loops are a *cis*-acting feature. A recent report described two stem-loops in the region of nt 1 to 51 and, of these, the second functions as a *cis*-replication element in the context of the MHV genome (24). (ii) SLIII (nt 97 to 116)

* Corresponding author. Mailing address: Department of Microbiology, University of Tennessee, Knoxville, TN 37996-0845. Phone: (865) 974-4030. Fax: (865) 974-4007. E-mail: dbrian@utk.edu.

† Present address: University of Tennessee, Chattanooga, Chattanooga, TN 37408.

‡ Present address: Crowder College, Neosho, MO 64850.

▽ Published ahead of print on 2 May 2007.

is predicted by both the Tinoco and Zuker algorithms, is supported by RNase structure probing, and appears to have a homolog in coronavirus groups 1 to 3 (34). In essentially all coronaviruses examined, a translation initiation codon for a short intra-5′ UTR open reading frame (ORF) of unknown function is associated with SLIII (34). Base covariations in the helical stem indicate that SLIII is phylogenetically conserved among group 2 coronaviruses (34 and data not shown). (iii) SLIV (nt 186 to 215) is a *cis*-acting phylogenetically conserved structure in group 2 coronaviruses with the exception of SARS-CoV (35). The structure of SLIV in SARS-CoV appears similar to those predicted for group 1 coronaviruses (35).

During initial studies to determine the structural requirements for BCoV DI RNA replication, it was learned that translation of the continuous ORF within the DI RNA was necessary for replication (7). Beyond this, it has not been determined how the partial nsp1 coding sequence functions in DI RNA replication. Interestingly, an analogous region of the nsp1 coding sequence is found in all naturally occurring and in one synthetically created coronavirus DI RNAs described to date (reviewed in reference 3). In addition, in the context of the MHV genome, a deletion of the 5′-proximal region of the nsp1 coding sequence, but not of the 3′-proximal region, prevents genome replication as determined through reverse genetics analyses (6). The mechanistic contribution of this sequence was not determined, but it was speculated to be perhaps a function of the protein product, an RNA structure, or both (6).

In this study, we have examined the function of the 5′-proximal 288 nt of the nsp1 coding region in the DI RNA ORF that provides replication competence to the BCoV DI RNA. We observed that (i) the 5′-terminal 186 nt of the nsp1 coding region are necessary and sufficient for DI RNA replication, (ii) within the 186-nt sequence are found two *Mfold*-predicted stem-loops, named SLV (nt 239 to 310) and SLVI (nt 311 to 340), that are supported by RNase structure probing and by nucleotide covariations that maintain the helical stems among the closely related group 2 coronaviruses, and (iii) SLVI is a required higher-order structure for DI RNA replication on the basis of mutation analyses. The function of SLV has not been evaluated. We conclude that SLVI within the BCoV nsp1 coding region acts as a higher-order *cis*-replication element for DI RNA and postulate that it functions similarly in the viral genome.

MATERIALS AND METHODS

Cells, virus, and DI RNA. A DI RNA-free stock of the Mebus strain of BCoV (genome sequence; GenBank accession no. U00735) at 4.5×10^8 PFU/ml was used as a helper virus as described previously (7, 8). The human rectal tumor cell line HRT-18 (43) was used in all experiments. pDrep1 is a pGEM3Zf(-) (Promega)-based plasmid containing the cDNA clone of a naturally occurring 2.2-kb DI RNA of BCoV modified to carry a 30-nt in-frame reporter (Fig. 1A) (8).

Enzyme structure probing of in vitro-transcribed RNA. RNA secondary structure modeling was performed using *Mfold* version 3.2 at http://www.bioinfo.rpi.edu/applications/mfold/ (31, 49). Enzyme structure probing was carried out as described elsewhere (37). Briefly, for in vitro synthesis of RNA, 10 μg of XbaI-linearized mung bean nuclease blunt-ended pDrep1 DNA (Fig. 1A) in a 200-μl reaction volume was transcribed at 37°C for 1 h using 80 U of T7 RNA polymerase (Promega). A yield of ~40 μg of a 595-nt-long vector-free transcript was obtained. RNA was treated with 10 U of RNase-free DNase (Promega) at 37°C for 30 min, extracted with phenol-chloroform, chromatographed through a Biospin 6 column (Bio-Rad), spectrophotometrically quantified, and stored in water at −20°C. For RNase treatments, 40 μg of RNA was heat denatured at 65°C for 3 min and renatured by slow cooling (0.5 h) to 35°C in a 400-μl reaction volume containing 30 mM Tris HCl (pH 7.5)–20 mM $MgCl_2$–300 mM KCl, and aliquots containing 2 μg of sample RNA and 10 μg of yeast tRNA were incubated in 100 μl of the same buffer and 1.0, 0.1, 0.05, 0.01, or 0.001 U of RNase CV1 (Pharmacia) or 5.0, 1.0, or 0.1 U of RNase T_2 (GIBCO), as noted below in the legend to Fig. 3. RNase digestion was carried out at 25°C for 15 min and terminated by the addition of 150 μl of 0.5 M sodium acetate, after which the RNA was extracted with phenol-chloroform and ethanol precipitated. Digested RNA preparations were used in primer extension reactions with 5′-end-labeled plus-strand-binding primer 1 (BCoV332-352 for mapping SLV) or primer 2 (BCoV379-400 for mapping SLVI) (Table 1). Undigested RNA was used with the same primers to identify natural reverse transcription stops and in dideoxynucleotidyl sequencing reactions to mark nucleotide positions. Products were analyzed on a DNA sequencing gel of 6% polyacrylamide.

Construction of mutant DI RNAs. Plasmids from which mutant DI RNAs were transcribed in vitro were modifications of pDrep1 (8). Modifications of pDrep1 were made by overlap PCR mutagenesis (19, 38, 45) using pDrep1 DNA template and the oligonucleotide primers described in Table 1. Restriction endonuclease sites used for final construction of the mutant plasmids are shown in Fig. 1A. Mutated regions were confirmed by sequencing.

To make p77Drep, the 210-nt 5′ UTR in pDrep1 was shortened by overlap mutagenesis wherein the products from primers PGEM3Z2097(-), BCoV47-74(+), DI211-232(-), and oligo 2(+) were extended, and the mutated 1,158-nt NdeI fragment from the extended product (the upstream NdeI site is within the vector) was used to replace the analogous fragment in pDrep1. To make p210Nrep, pNrep2 (8) was digested with BglII, and the resulting 754-nt BglII fragment was used to replace the analogous fragment in pDrep1.

3′-end deletions of the 288-nt partial nsp1 coding region within pDrep1 were made by overlap PCR mutagenesis wherein primers Nstart(-) and oligo 2(+) were used to make the 3′-proximal overlapping fragment and primers PGEM3Z2477(-) and the indicated mutant primers (Table 1) were used to make the 5′-proximal overlapping fragments of differing lengths. The mutated HpaI-XbaI fragments from the final extended PCR products were used to replace the analogous fragment in pDrep1. The name of each deletion mutant corresponds to the primer used with the same name.

pLeftVI was made by PCR overlap mutagenesis wherein primers PGEM3Z2477(-), Leftvi(+), Leftvi(-), and oligo 2(+) were used to make an overlap PCR product from which the mutated 1,158-nt NdeI fragment was used to replace the analogous fragment in pDrepl. pRightVI was made in the same way except for the use of primers Rightvi(+) and Rightvi(-), respectively.

In vitro translation. For in vitro translation, ~2 μg of transcript was translated in a 50-μl reaction mix containing 35 μl of rabbit reticulocyte lysate (Promega) and 20 μCi of [^{35}S]methionine (>800 Ci/mmol; MP Biochemicals) as recommended by the manufacturer. Radiolabeled proteins were resolved by sodium dodecyl sulfate-polyacrylamide gel electrophoresis in gels of 12% polyacrylamide (Tris-HCl Ready gel; Bio-Rad) by the method of Laemmli (25), and dried gels were exposed to Kodak XAR-5 film for imaging.

Northern assay for DI RNA replication. The Northern assay for detecting reporter-containing DI RNAs was performed as described previously (8, 33). Briefly, 5 μg of MluI-linearized plasmid DNA was blunt ended with mung bean nuclease and transcribed with 40 U of T7 RNA polymerase (Promega) in a 100-μl reaction mixture to produce uncapped DI RNA. The reaction mix was treated with 5 U of RNase-free DNase (Promega), and RNA was chromatographed through a Biospin 6 column (Bio-Rad) and quantitated spectrophotometrically. Cells (~6×10^6) at ~80% confluence in a 35-mm dish were infected with BCoV at a multiplicity of 10 PFU per cell and transfected 1 h later with 1 μg of RNA using Lipofectin (Bethesda Research Laboratories). At the indicated times postinfection, RNA (approximately 10 μg per plate) was extracted by the Nonidet P-40–proteinase K method (8) and stored as an ethanol precipitate. For passage of progeny virus, supernatant fluids were harvested at 48 h postinfection (hpi), and 500 μl was used to infect freshly confluent cells (~8×10^6) in a 35-mm dish from which RNA was extracted at 48 hpi. For electrophoretic separation of RNA in a formaldehyde-agarose gel, 2.5 μg per lane was used. Approximately 1 ng of transcript, identified as RNA in the Northern blot figures, was loaded per lane when used as a marker. RNA was transferred to Nytran membrane by vacuum blotting, and the UV-irradiated blots were probed with oligonucleotide TGEV(+) that had been 5′-end labeled with ^{32}P to specific activities of 1×10^6 to 4×10^7 cpm/pmol. Probed blots were exposed to Kodak XAR-5 film for 1 to 7 days at −80°C for imaging.

Reverse transcription-PCR and sequence analysis of mutant DI RNA replicons. With RNA extracted from cells at 24 h postinfection with VP1 virus collected from mutant transfections, reverse transcription was done using DI

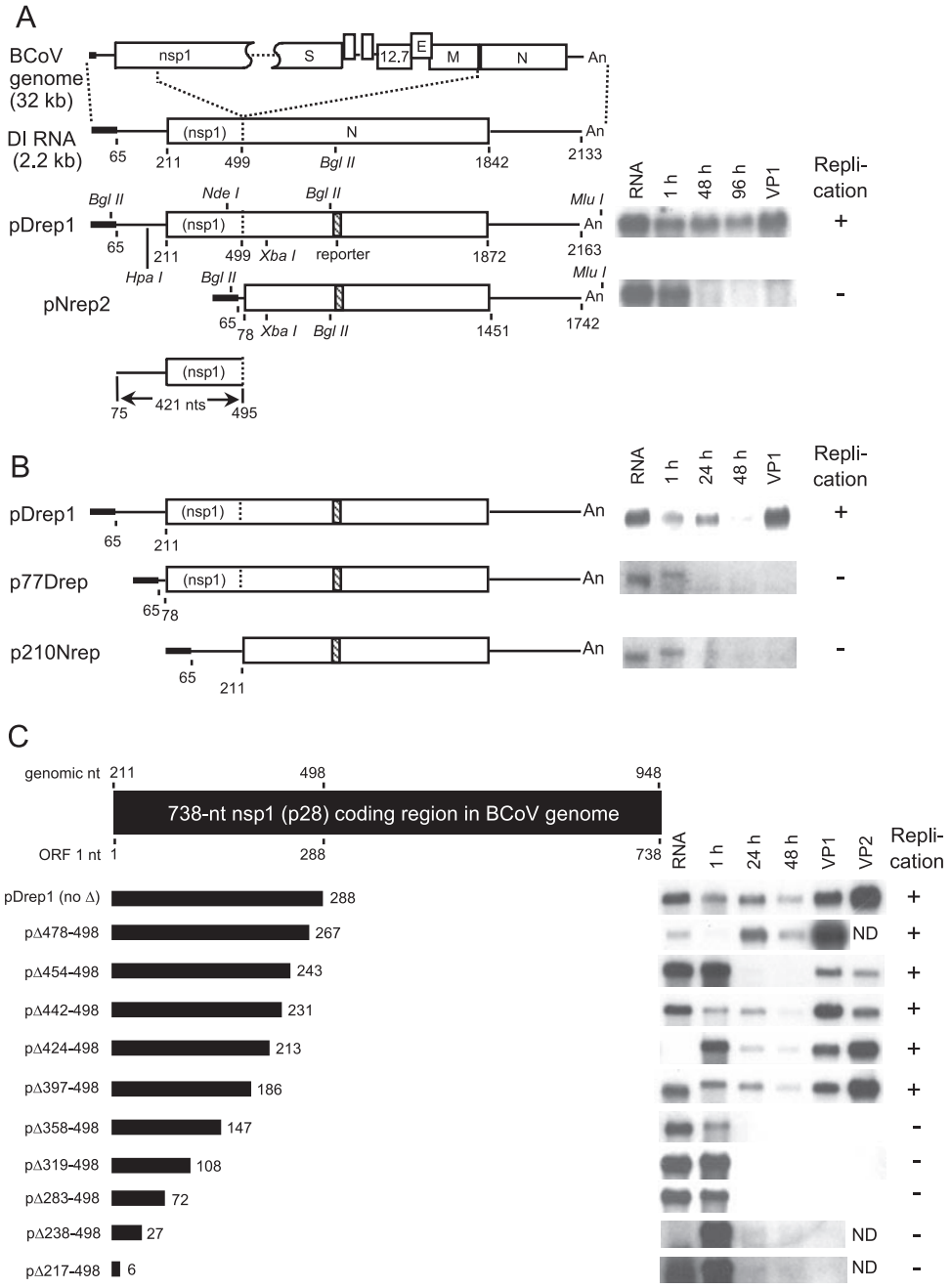

FIG. 1. Location of *cis*-replication elements within the partial nsp1 coding region in BCoV DI RNA. A. Structure of the naturally occurring BCoV DI RNA relative to the full-length BCoV genome. The DI RNA is composed of the fused ends of the viral genome as described in the text. The 65-nt leader is illustrated by a filled rectangle. The partial nsp1 sequence in parentheses represents the 5′-proximal 288 nt of the 738-nt nsp1 coding region. The cloned, modified BCoV DI RNA is under control of the T7 RNA polymerase promoter, carries a 30-nt in-frame reporter used for Northern probing, and is named pDrep1. Restriction endonuclease sites used for further engineering as described in this report are depicted. The cloned, modified BCoV N mRNA (mRNA 7) is under control of the same promoter as pDrep1, carries the same reporter, and is named pNrep2. The difference in the RNA transcripts from the two plasmids both linearized at the MluI site is a continuous sequence of 421 nt as depicted. At the right are shown the results of Northern analyses depicting the accumulation of pDrep1 RNA at 48 and 96 h posttransfection and at 24 hpi following first virus passage (VP1), and the absence of accumulation of the pNrep2 RNA. RNA, ~1 ng of transcript used for transfection. B. Structures of modified pDrep1 that carry the 5′ UTR of mRNA 7, named p77Drep, and the 5′ UTR of the genome but without the 288-nt region of nsp1, named p210Nrep. At the right are Northern analyses depicting the accumulation of wt DI RNA and the absence of accumulation for RNAs from p77Drep and p210Nrep. RNA, ~1 ng of transcript used for transfection. C. Deletion analysis of the 288-nt partial nsp1 coding region in BCoV DI RNA. 3′-terminal deletions of the partial nsp1 coding region were made as indicated, and RNAs from the mutants were tested for accumulation. The results of Northern analyses at the right illustrate that DI RNAs carrying the first 186 nt of nsp1 coding region accumulated, whereas those with less than 186 nt did not. RNA, ~1 ng of transcript used for transfection.

TABLE 1. Oligonucleotides used in this study

Oligonucleotide[a]	Polarity[b]	Sequence (5′→3′)	Binding region nt in pDrep[c]
1aΔ217-498 (+)	−	GAGTAAAAGACAT/CGACATTGTG	207–216/499–511
1aΔ238-498 (+)	−	GAGTAAAAGACAT/GAGACCGTATTTG	225–237/499–511
1aΔ283-498 (+)	−	GAGTAAAAGACAT/TCTGCGTCCTC	274–282/499–511
1aΔ319-498 (+)	−	GAGTAAAAGACAT/CACCTCTGAAC	308–318/499–511
1aΔ358-498 (+)	−	GAGTAAAAGACAT/TGTTTCCAGC	348–357/499–511
1aΔ397-498 (+)	−	GAGTAAAAGACAT/ACAATCCACCATC	384–396/499–511
1aΔ409-498 (+)	−	GAGTAAAAGACAT/AAGAAGTCGGC	398–408/499–511
1aΔ424-498 (+)	−	GAGTAAAAGACAT/ACAACACTCTTG	412–423/499–511
1aΔ442-498 (+)	−	GAGTAAAAGACAT/TATTAGGCTAG	431–441/499–511
1aΔ454-498 (+)	−	GAGTAAAAGACAT/AACAATTTCACG	442–453/499–511
1aΔ478-498 (+)	−	GAGTAAAAGACAT/CAAATCATATGGAC	464–477/499–511
BCoV47-74 (+)	−	TAAAGTTTAGATTATAAAAAGATCTAAC	47–74
BCoV332-352 (+)	−	CCAGCTTTTGCGCAGTGGTGG	332–352
BCoV379-400 (+)	−	GGCGACAATCCACCATCACATG	379–400
DI211-232 (−)	+	CGTATTTGTTGATCTTCGACAT/CCTTAAAGTTTAG	65–74/211–232
Leader7-32 (−)	+	GAGCGATTTGCGTGCGTGCATCCCGC	7–32
LeftVI (−)	+	GTAGTTCAGAAGTCGATATAGTATG	305–329
LeftVI (+)	−	CATACTATATCGACTTCTGAACTAG	305–329
Nstart (−)	+	ATGTCTTTTACTCCTGGTAAGC	499–520
Oligo2 (+)	−	GTCCCGATCGAGAATGTCAGCCGGGG	968–993
PGEM3Z2097 (−)	+	AGGGCGACACGGAAATGTTG	(2097–2116)[d]
PGEM3Z2477 (−)	+	GGCATCAGAGCAGATTGTACTG	(2477–2498)[d]
RightVI (−)	+	GATATAGTATGCTCGACTACTGCGC	319–343
RightVI (+)	−	GCGCAGTAGTCGAGCATACTATATC	319–343
TGEV 8 (+)	−	CATGGCACCATCCTTGGCAACCCAGA	1098–1123

[a] The positive and negative symbols in oligonucleotide names indicate the polarity of the nucleic acid to which the oligonucleotide anneals.
[b] Polarity of the oligonucleotide relative to the positive-strand DI RNA.
[c] For probe binding to negative-strand sequence, the numbers given correspond to complementary positive-strand sequence.
[d] Binds in the pGEM3Zf(-) vector upstream of the DI RNA transcription start site.

RNA-specific primer TGEV(+), PCR was done using primers TGEV(+) and leader(-), and the PCR product was sequenced directly.

RESULTS

The 288-nt partial nsp1 coding region provides a required function for BCoV DI RNA replication. Previous studies had demonstrated that a T7 RNA polymerase-generated sgmRNA 7 (mRNA for the N protein) of BCoV containing a short reporter sequence does not replicate when transfected into BCoV-infected cells, whereas the DI RNA containing the same reporter sequence does (8). The difference between the two molecules is a continuous stretch of 421 nt that is made up of some of the genomic 5′ UTR sequence and all of the 288-nt partial nsp1 region (Fig. 1A). To test whether the genomic 5′ UTR and the partial nsp1 coding region independently fulfill requirements for replication of the DI RNA, constructs were made to test each domain separately. In the first, the 210-nt DI RNA 5′ UTR was precisely replaced with the 77 5′ UTR of sgmRNA 7, resulting in p77Drep, which lacks 136 nt of the genomic 5′ UTR but retains the 288-nt partial nsp1 coding region. Transcripts of p77Drep were then tested for replication in helper virus-infected cells (Fig. 1B). Accumulation of DI RNA by 24 and 48 h posttransfection, and by 24 hpi following infection with first virus passage (VP1), were used as evidence of DI RNA replication (8, 34, 35, 45). As shown in Fig. 1B, this molecule failed to replicate, indicating signals necessary for replication are missing. This result has been confirmed and extended by experiments showing requirements for both SLIII and SLIV (mapping between nt 97 and 210) in DI RNA replication (34, 35). In the second construct, the 77-nt 5′ UTR of the reporter-containing mRNA 7 construct (pNrep2) (8) was precisely replaced with the 210-nt genomic 5′ UTR, forming p210Nrep. From this plasmid, a DI RNA-like molecule was made that had the 210-nt genomic 5′ UTR and all the N-coding domain and reporter sequence but was missing the entire 5′-proximal 288 nt of the nsp1 coding domain. Figure 1B illustrates that a transcript of p210Nrep also failed to replicate in helper virus-infected cells, thus demonstrating a requirement for all or part of the 288-nt partial nsp1 coding region in the DI RNA for replication.

***cis*-acting signals for DI RNA replication map within the 5′-terminal 186 nt of the partial nsp1 coding region in the DI RNA, a region containing SLV and SLVI.** To characterize the *cis*-acting features within the 288-nt partial nsp1 coding region, conserved sequences and higher-order structures among eight group 2 coronaviruses previously studied (BCoV-Mebus, human coronavirus [HCoV]-OC43, HCoV-4408, porcine hemagglutinating encephalomyocarditis [HEV]-TN11, equine coronavirus [ECoV]-NC99, classed as BCoV-like, and mouse hepatitis coronavirus [MHV-A59, MHV-2, and MHV-JHM], classed as MHV-like [46]), were identified and treated as potential *cis*-acting elements. For this, sequences were aligned (46) and the *Mfold* program of Zuker applied to each. Four predicted hairpin stem-loops showing nucleotide variations in the helical stems among the eight viruses were identified and named SLV through SLVIII (Fig. 2). This nomenclature continues that used for BCoV 5′-proximal stem-loops (7, 8, 34, 35). In BCoV, SLV maps at nt 239 to 310, SLVI at nt 311 to 340, SLVII at nt 356 to 373, and SLVIII at nt 378 to 446, and the calculated free energies are −27.1, −10.9, −2.9, and −26.4

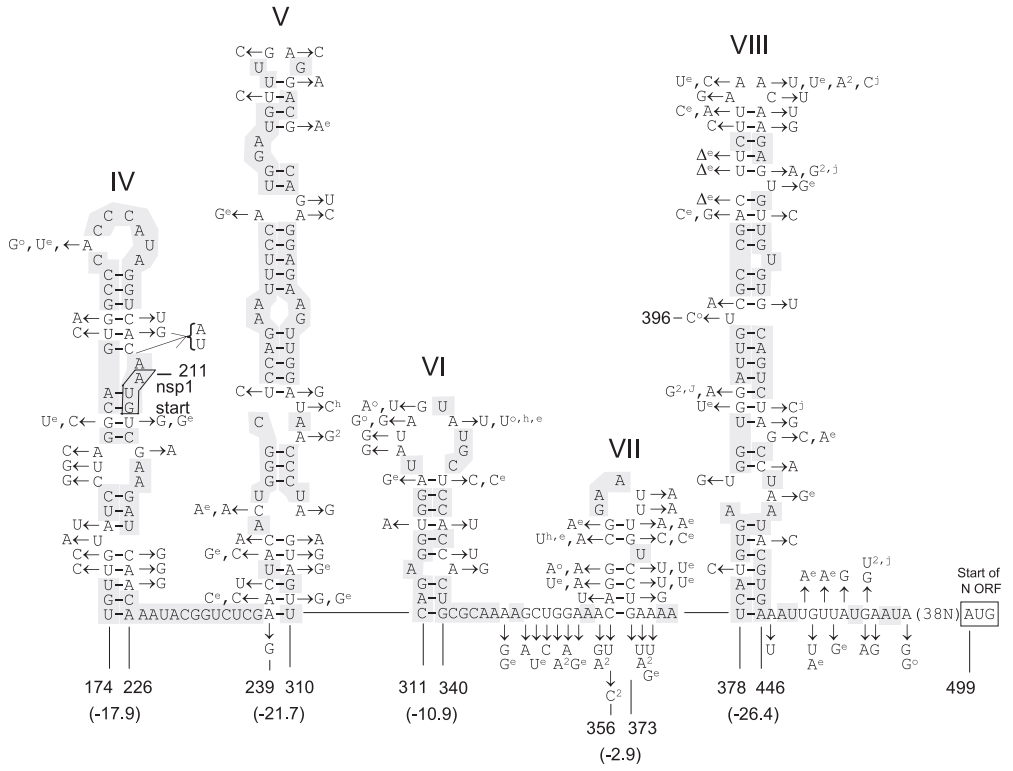

FIG. 2. Stem-loops in the 5′-proximal 288 nt of the 738-nt nsp1 coding region as predicted by *Mfold*. Named nucleotides are those in BCoV. Unless otherwise indicated, they are also the nucleotides in the other named group 2 coronaviruses and are highlighted in gray. Arrows identify bases in MHV-A59, MHV-2, and MHV-JHM unless otherwise identified by superscipts. The compared group 2 coronaviruses and their superscript designations, if any, are BCoV-Mebus, HCoV-OC43 (o), HCoV-4408, HEV-TN11 (h), ECoV-NC99 (e), MHV-A59 (a), MHV-2 (2), and MHV-JHM (j). The free energies noted refer to the stem-loops in the BCoV RNA.

kCal/mol, respectively (Fig. 2). Identical bases aligning among the eight coronaviruses are shown in Fig. 2, and those that differ are identified. Although the SARS-CoV has been classified as a group 2 coronavirus (41), structural homologues of stem-loops V to VIII in SARS-CoV were not apparent by these analyses (data not shown).

To determine whether the entire nsp1 portion present in the DI RNA molecule is required for DI RNA replication, a set of 3′-terminal in-frame deletions of this region in pDrep1 was made by overlap PCR mutagenesis, and T7 RNA polymerase-generated transcripts of each mutant were tested for replication in helper virus-infected cells. Figure 1C summarizes the data showing that deletion mutants 1aΔ478-498 through 1aΔ397-498 replicated, as evidenced by accumulation of DI RNA after VP1 and VP2, whereas 1aΔ358-498 through 1aΔ217-498 did not. A low level of DI RNA accumulation prior to virus passage posttransfection (for example, the undetectable amounts for mutant p454-498 at 24 h and 48 h posttransfection in Fig. 1C) may reflect structural influences on replication, but we noted that amounts of accumulation at these times did vary widely, even for wt DI RNA (e.g., compare Fig. 1 and 4, below). Thus, for DI RNA replication, the 3′-terminal 102 nt of the 288-nt partial nsp1 coding region, which contains most of SLVIII, are not needed. It was therefore concluded that the SLV- to SLVII-containing 5′-proximal 186-nt region contains one or more *cis*-acting elements required for DI RNA replication. Of these, SLV and SLVI were chosen for further analysis since they possessed relatively low free energies and demonstrated sequence conservation in the stems.

RNase structure maps are consistent with predicted stem-loops V and VI. To determine whether stem-loops V and VI as predicted by *Mfold* are supported by enzyme structure probing, synthetic transcripts of the first 288 nt of the nsp1 coding region were probed by methods used previously to analyze stem-loops I through IV and the 3′-proximal pseudoknot (9, 34, 35, 45). For this, pDrep1 was linearized at the XbaI site and T7 RNA polymerase-generated transcripts were digested with various concentrations of RNase specific for single-stranded regions (RNase T_2 [nonspecific with a preference for A]) and helical regions (cobra venom RNase V1). The positions of cleavage sites in the RNA (summarized in Fig. 3A) were determined by analyzing primer extension products in parallel with a dideoxy sequencing ladder generated from untreated RNA (Fig. 3B and C). Primer extension products of uncut RNA were also examined to identify natural reverse transcription stops. The results showed that for SLV via extension of primer 1 (Fig. 3B), strong single-strand hits were present at nt 227 to 230, a predicted single-stranded region between SLIV and SLV, at nt 268 and 269, sites within and adjacent to a predicted 2-nt bulge, and at nt 273 to 276, sites within the predicted 4-nt terminal loop. In addition, weak single-strand hits were observed at nt 267, a site within a 2-nt bulge, at nt 272, a site adjacent to the terminal loop, at nt 282, a site

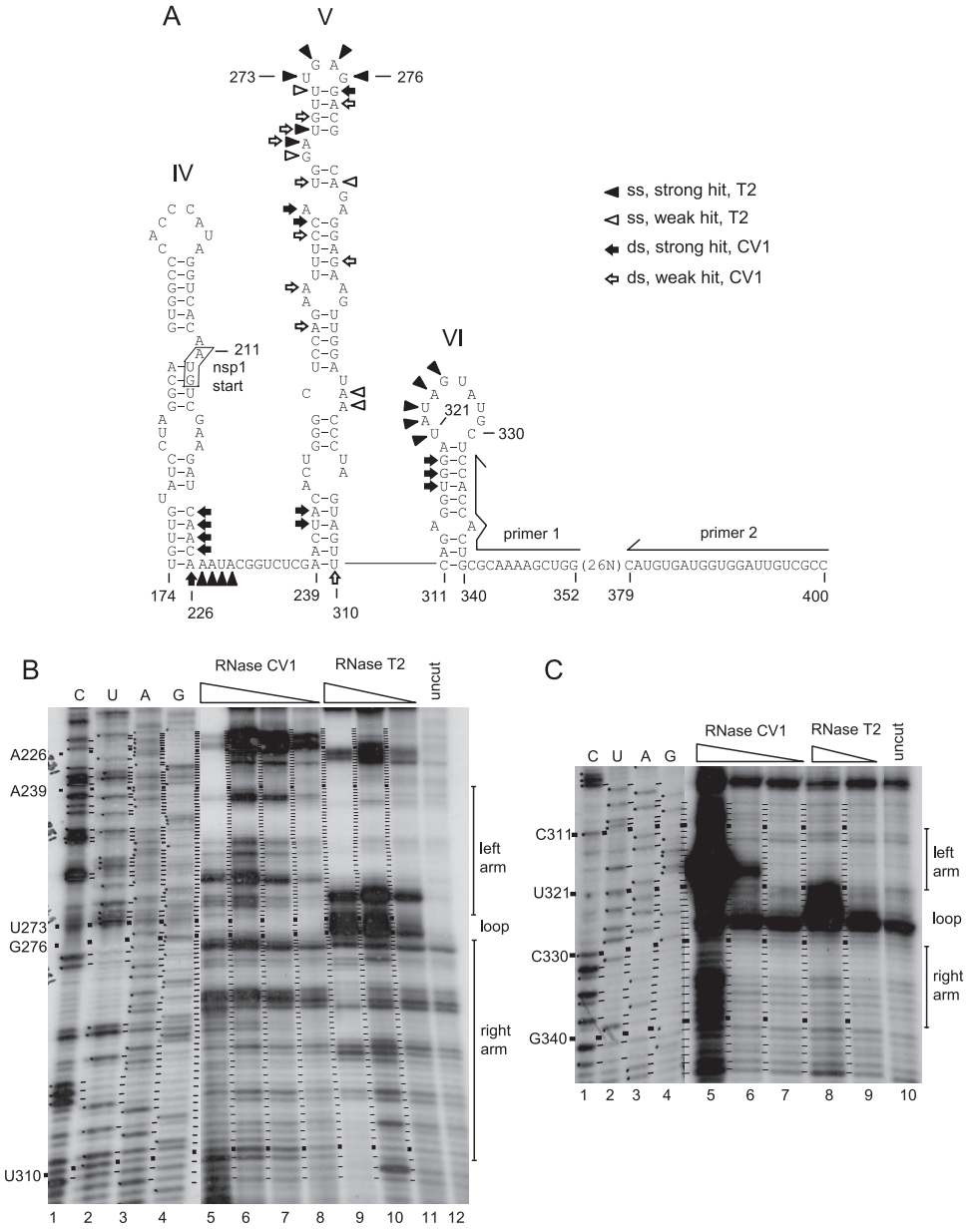

FIG. 3. Enzyme structure probing of SLV and SLVI in BCoV. A. Schematic summary of structure probing data. B. Electrophoretic analysis of digestion products in the SLV region from extensions of primer 1. Lanes 1 through 4, sequencing ladder generated from primer 1; lanes 5 through 8, RNase CV_1 digestion with 1.0, 0.1, 0.05, and 0.01 U, respectively; lanes 9 through 11, RNase T_2 digestion with 5.0, 1.0, and 0.1 U, respectively; lane 12, undigested RNA. C. Electrophoretic analysis of digestion products in the SLVI region from extensions of primer 2. Lanes 1 through 4, sequencing ladder generated from primer 2; lanes 5 through 7, RNase CV_1 digestion with 0.1, 0.01, and 0.01 U, respectively; lanes 8 and 9, RNase T_2 digestion with 1.0 and 0.1 U, respectively.

adjacent to an internal loop, and at nt 298 and 299, sites within a predicted internal loop. Strong double-strand hits were present at nt 222 to 226, a previously unmapped region that appears to extend the length of SLIV described earlier (35) (to be analyzed further elsewhere). Strong double-strand hits were also present at nt 242 and 243, a predicted double-stranded region, at nt 263 and 264, adjacent to and within an internal loop, and at nt 277, adjacent to the terminal loop. In addition, weak double-strand hits were observed within stems at nt 255, 262, 265, 269, 270, 278, 288, and 310 and within loop regions at nt 258 and 268. Double-strand hits in predicted loop regions may be explained by the fact that CV1 on occasion digests within single-stranded regions, adopting an approximately helical conformation (27).

The mapping results for SLVI as observed via extension of primer 2 (Fig. 3C) show strong single-strand hits at nt 321 to 325, which represent 5 of the 10 nt in the predicted terminal loop. Strong double-strand hits were present at nt 317 to 319, a region predicted to be in the upper stem.

Thus, RNase probing with T_2 and CV1 RNases overall

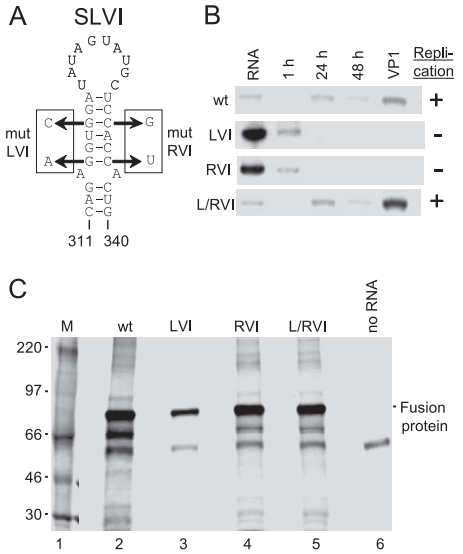

FIG. 4. Effects of SLVI mutations on accumulation of BCoV DI RNA. A. Mutations used to test the *cis*-requirement of SLVI for DI RNA replication. B. Northern analysis to measure the accumulation of wt and SLVI mutant DI RNAs. The ^{32}P-labeled oligonucleotide probe specific for the 30-nt TGEV reporter sequence in the DI RNAs was used. RNA, ~1 ng of transcript used for transfection. C. Translation of wt and mutant DI RNAs. T7 RNA polymerase-generated transcripts of wt and mutant DI RNA were translated in rabbit reticulocyte lysate in the presence of ^{35}S-labeled methionine, and the dried gel was autoradiographed. Lane 1, high-molecular-weight Rainbow marker proteins (Amersham); lane 6, translation product from a reaction mixture to which no RNA was added.

yielded results consistent with the stem-loop V and VI structures predicted by *Mfold*.

Mutation analyses show that SLVI plays a functional role in DI RNA replication. Between SLV and SLVI, SLVI was chosen for testing a *cis*-replication function since it is relatively small and lends itself to translationally silent stem-disrupting nucleotide changes. It also demonstrated a high level of nucleotide sequence conservation in its upper stem compared with other group 2 coronaviruses (46) (Fig. 2).

To test the replication function of SLVI, base substitutions were made in the third (wobble) nucleotide positions of four base-paired codons in the upper stem that were predicted to disrupt helical structure but preserve wild-type amino acid sequence (Fig. 4A). In construct pLeftVI, substitutions 315G→A and 318G→C were made, and following transfection of transcripts into virus-infected cells no DI RNA accumulation was observed at 24 and 48 h posttransfection, nor was replication observed at 24 h following the first passage of virus (Fig. 4B, LVI). Likewise, when mutations 333C→G and 336C→T were made to form pRightVI, no replication was observed (Fig. 4B, RVI). However, when compensatory restoration of stem-loop VI was made by combining the mutations in pLeftVI and pRightVI, replicating ability was restored as evidenced by the accumulation of DI RNA at 24 and 48 h posttransfection and by replication following the first virus passage (Fig. 4B, L/RVI). Sequence analysis of cDNA clones made from VP1 RNA of the replicating L/RVI double mutant demonstrated that all four mutations were retained (data not shown).

Since the mutations made in SLVI resulted in codons used in the BCoV genome (57% of the time for GAA [Glu], 8% of the time for GUC [Val], 2.6% of the time [19 times total] for UCG [Ser], and 48% of the time for ACU [Thr]), it was not anticipated that blocks in DI RNA replication would result from failed translation of the mutated DI RNA ORFs. To establish that translation was not blocked by the mutations, transcripts of the mutant DI RNAs were translated in rabbit reticulocyte lysate, and the products were examined. The results shown in Fig. 4C demonstrate that wt and all three mutant forms of DI RNA are translated to generate the fused DI RNA ORF product of approximately 62 kDa. The apparent larger size for this protein is due to its phosphorylation (data not shown).

From these combined results, it was concluded that stem-loop VI, as a higher-order structure, is a required *cis*-acting element for BCoV DI RNA replication.

Whether SLV functions similarly remains to be determined.

DISCUSSION

In the current study, we report the existence of a higher-order RNA structure identified as SLVI within the nsp1 coding region of the coronaviral genome that appears to act directly in *cis* for DI RNA replication. SLVI maps within a part of the nsp1 coding region found in all naturally occurring coronavirus DI RNAs (3, 4, 8) and in one synthetic MHV-A59 DI RNA (30) described to date, suggesting that a structure analogous to SLVI may be required for the replication of these DI RNAs as well. In at least one other instance, an apparently directly acting higher-order *cis*-replication structure has been found to map within the coding region of a coronavirus DI RNA. In that case, the structure, a 55-nt stem-loop derived from the nsp 3 ORF, exists in a subset of multipartite DI RNAs generated from MHV-JHM (36). Other *cis*-acting RNA structures have been mapped within the coding region of the coronavirus genome but appear to function indirectly in genome replication (29). These include the ribosome frameshifting pseudoknot located just downstream of the ORF 1a/1b junction (5, 13), the (usually) intergenic core sequence (also called the transcription regulatory sequence) associated with RdRp template switching during formation of sgmRNA templates (50), and a genome packaging signal that maps within ORF 2b (11). A *cis*-replication element has been described within a coding region of an arterivirus (2, 44), a virus group that along with coronaviruses, toroviruses, and roniviruses is a member of the *Nidovirus* group. This *cis*-acting structure is in the 3′-proximal region of the arterivirus genome, however, and to date appears not to have a homolog in the coronavirus genome.

Whether SLVI is the only directly acting *cis* RNA replication element within the 5′-terminal region of ORF 1a remains to be determined. SLV is a complex stem-loop that shows considerable structural conservation among the group 2 coronaviruses but has yet to be examined for a *cis*-replication function. Curiously, like SLVI, the terminal loop of SLV appears to be the most variable part of its structure. The proximity of SLV and SLVI suggests they may be components of a single larger *cis*-acting structure.

It also remains to be determined what role the protein moiety of the partial nsp1 product plays as a *cis*-acting feature, if

any. It was initially thought that translation of the partial ORF 1a sequence in the BCoV DI RNA is also required for replication (7). Replacing the AUG start codon for the partial nsp1 ORF in DI RNA with a UAG stop codon resulted in no DI RNA replication, even when the N portion of the DI RNA ORF remained open (7). The notion that translation of the partial nsp1 ORF is required for DI RNA replication has been supported by two additional experiments in which the amino acid composition within short regions of the partial nsp1 product was changed and tested. In the first mutant, a nucleotide deletion at position 223 (causing a −1 frameshift) and a nucleotide insertion at position 304 (causing a +1 frameshift) caused amino acids 5 through 31 to change from 5NKYGLE LHWAPEFPWMFEDAEEKLDNP31 in the wt DI RNA to 5TNTVSNYTGLQNFHGCLRTQRRSWITL31 in the mutant. In the second mutant, a nucleotide deletion at position 270 (causing a −1 frameshift) and a nucleotide insertion at position 304 (causing a +1 frameshift) caused amino acids 20 through 31 to change from 20MFEDAEEKLDNP31 in the wt DI RNA to 20CLRTQRRSWITL31 in the mutant. Both of these mutations map within the region of SLV. Neither mutant replicated (data not shown). Thus, it could be that a feature of the translated partial nsp1 product fulfills a *cis*-requirement for replication, but it cannot be ruled out at this time that the nucleotide insertions and deletions altered a required *cis*-acting RNA structure.

To date, nsp1 has been the most characterized in MHV and SARS-CoV. In MHV, nsp1 is a 28-kDa protein, also called p28, the first proteolytically cleaved product of the polyprotein synthesized from ORF 1a (12). When p28 is expressed in the absence of the other viral proteins, it has profound effects on cell metabolism, including the induction of cell cycle arrest at G_0/G_1 (10). Interestingly, by using reverse genetics it was shown that the C-terminal region of p28 is not absolutely required for virus replication but that deletion of the N-terminal region is lethal for the virus (6). Expression of the SARS-CoV nsp1 protein alone in cells promoted host mRNA degradation (23).

The identification of *cis*-replication elements in the large coronavirus genome remains a technical challenge but is now approachable with the use of reverse genetics systems (reviewed in reference 29). An important caveat when using DI RNAs for this identification is that such elements might be idiosyncratic for the DI RNA genome. One example of this is the coronavirus common octamer (GGAAGAGC) in the 3′ UTR which functions as a *cis*-replication element in DI RNA but not in the full-length genome (15). On the basis of the work presented here, we suggest that the presence of a *cis*-acting element for genome replication mapping within the 5′-proximal region of nsp1 may be one reason the 5′-proximal region of nsp1 cannot be deleted from the intact MHV genome (6). The presence of a *cis*-acting element within the partial nsp1 coding region along with SLIII and -IV in the BCoV 5′ UTR could also explain why it is that the sgmRNAs produced by this virus, although they are found in double-stranded RNA-synthesizing transcriptive intermediates (1, 37), are not replicating molecules as once postulated (17, 39, 40).

ACKNOWLEDGMENTS

This work was supported by Public Health Service grant AI14267 from the National Institute of Allergy and Infectious Diseases and by funds from the University of Tennessee, College of Veterinary Medicine, Center of Excellence Program for Livestock Diseases and Human Health.

REFERENCES

1. **Baric, R. S., and B. Yount.** 2000. Subgenomic negative-strand RNA function during mouse hepatitis virus infection. J. Virol. **74:**4039–4046.
2. **Beerens, N., and E. J. Snijder.** 2006. RNA signals in the 3′ terminus of the genome of equine arteritis virus are required for viral RNA synthesis. J. Gen. Virol. **87:**1977–1983.
3. **Brian, D. A., and R. S. Baric.** 2005. Coronavirus genome structure and replication. Curr. Top. Microbiol. Immunol. **287:**1–30.
4. **Brian, D. A., and W. J. M. Spaan.** 1997. Recombination and coronavirus defective interfering RNAs. Semin. Virol. **8:**101–111.
5. **Brierley, I., M. E. Boursnell, M. M. Binns, B. Bilimoria, V. C. Blok, T. D. Brown, and S. C. Inglis.** 1987. An efficient ribosomal frame-shifting signal in the polymerase-encoding region of the coronavirus IBV. EMBO J. **6:**3779–3785.
6. **Brockway, S. M., and M. R. Denison.** 2005. Mutagenesis of the murine hepatitis virus nsp1-coding region identifies residues important for protein processing, viral RNA synthesis, and viral replication. Virology **340:**209–223.
7. **Chang, R. Y., and D. A. Brian.** 1996. *cis* requirement for N-specific protein sequence in bovine coronavirus defective interfering RNA replication. J. Virol. **70:**2201–2207.
8. **Chang, R. Y., M. A. Hofmann, P. B. Sethna, and D. A. Brian.** 1994. A *cis*-acting function for the coronavirus leader in defective interfering RNA replication. J. Virol. **68:**8223–8231.
9. **Chang, R. Y., R. Krishnan, and D. A. Brian.** 1996. The UCUAAAC promoter motif is not required for high-frequency leader recombination in bovine coronavirus defective interfering RNA. J. Virol. **70:**2720–2729.
10. **Chen, C. J., K. Sugiyama, H. Kubo, C. Huang, and S. Makino.** 2004. Murine coronavirus nonstructural protein p28 arrests cell cycle in G_0/G_1 phase. J. Virol. **78:**10410–10419.
11. **Cologna, R., and B. G. Hogue.** 2000. Identification of a bovine coronavirus packaging signal. J. Virol. **74:**580–583.
12. **Denison, M. R., P. W. Zoltick, J. L. Leibowitz, C. J. Pachuk, and S. R. Weiss.** 1991. Identification of polypeptides encoded in open reading frame 1b of the putative polymerase gene of the murine coronavirus mouse hepatitis virus A59. J. Virol. **65:**3076–3082.
13. **Dos Ramos, F., M. Carrasco, T. Doyle, and I. Brierley.** 2004. Programmed −1 ribosomal frameshifting in the SARS coronavirus. Biochem. Soc. Trans. **32:**1081–1083.
14. **Goebel, S. J., B. Hsue, T. F. Dombrowski, and P. S. Masters.** 2004. Characterization of the RNA components of a putative molecular switch in the 3′ untranslated region of the murine coronavirus genome. J. Virol. **78:**669–682.
15. **Goebel, S. J., T. B. Miller, C. J. Bennett, K. A. Bernard, and P. S. Masters.** 2007. A hypervariable region within the 3′ *cis*-acting element of the murine coronavirus genome is nonessential for RNA synthesis but affects pathogenesis. J. Virol. **81:**1274–1287.
16. **Goebel, S. J., J. Taylor, and P. S. Masters.** 2004. The 3′ *cis*-acting genomic replication element of the severe acute respiratory syndrome coronavirus can function in the murine coronavirus genome. J. Virol. **78:**7846–7851.
17. **Hofmann, M. A., P. B. Sethna, and D. A. Brian.** 1990. Bovine coronavirus mRNA replication continues throughout persistent infection in cell culture. J. Virol. **64:**4108–4114.
18. **Holland, J. J.** 1985. Generation and replication of defective viral genomes, p. 77–99. *In* B. N. Fields (ed.), Fields virology, 1st ed. Raven Press, New York, NY.
19. **Horton, R. M., C. Zeling, N. H. Steffan, and L. R. Bease.** 1990. Gene splicing by overlap extension: tailor-made genes using polymerase chain reaction. BioTechniques **8:**528–535.
20. **Hsue, B., T. Hartshorne, and P. S. Masters.** 2000. Characterization of an essential RNA secondary structure in the 3′ untranslated region of the murine coronavirus genome. J. Virol. **74:**6911–6921.
21. **Hsue, B., and P. S. Masters.** 1997. A bulged stem-loop structure in the 3′ untranslated region of the genome of the coronavirus mouse hepatitis virus is essential for replication. J. Virol. **71:**7567–7578.
22. **Hsue, B., and P. S. Masters.** 1998. An essential secondary structure in the 3′ untranslated region of the mouse hepatitis virus genome. Adv. Exp. Med. Biol. **440:**297–302.
23. **Kamitani, W., K. Narayanan, C. Huang, K. Lokugamage, T. Ikegami, N. Ito, H. Kubo, and S. Makino.** 2006. Severe acute respiratory syndrome coronavirus nsp1 protein suppresses host gene expression by promoting host mRNA degradation. Proc. Natl. Acad. Sci. USA **103:**12885–12890.
24. **Kang, H., M. Feng, M. E. Schroeder, D. P. Giedroc, and J. L. Leibowitz.** 2006. Putative *cis*-acting stem-loops in the 5′ untranslated region of the

severe acute respiratory syndrome coronavirus can substitute for their mouse hepatitis virus counterparts. J. Virol. **80:**10600–10614.
25. **Laemmli, U. K.** 1970. Cleavage of structural proteins during the assembly of the head of bacteriophage T4. Nature **227:**680–685.
26. **Levis, R., B. G. Weiss, M. Tsiang, H. Huang, and S. Schlesinger.** 1986. Deletion mapping of Sindbis virus DI RNAs derived from cDNAs defines the sequences essential for replication and packaging. Cell **44:**137–145.
27. **Lowman, H. B., and D. E. Draper.** 1986. On the recognition of helical RNA by cobra venom V1 nuclease. J. Biol. Chem. **261:**5396–5403.
28. **Makino, S., and M. M. Lai.** 1989. High-frequency leader sequence switching during coronavirus defective interfering RNA replication. J. Virol. **63:**5285–5292.
29. **Masters, P. S.** 2006. The molecular biology of coronaviruses. Adv. Virus Res. **66:**193–292.
30. **Masters, P. S., C. A. Koetzner, C. A. Kerr, and Y. Heo.** 1994. Optimization of targeted RNA recombination and mapping of a novel nucleocapsid gene mutation in the coronavirus mouse hepatitis virus. J. Virol. **68:**328–337.
31. **Mathews, D. H., M. D. Disney, J. L. Childs, S. J. Schroeder, M. Zuker, and D. H. Turner.** 2004. Incorporating chemical modification constraints into a dynamic programming algorithm for prediction of RNA secondary structure. Proc. Natl. Acad. Sci. USA **101:**7287–7292.
32. **Nanda, S. K., and J. L. Leibowitz.** 2001. Mitochondrial aconitase binds to the 3′ untranslated region of the mouse hepatitis virus genome. J. Virol. **75:** 3352–3362.
33. **Ozdarendeli, A., S. Ku, S. Rochat, G. D. Williams, S. D. Senanayake, and D. A. Brian.** 2001. Downstream sequences influence the choice between a naturally occurring noncanonical and closely positioned upstream canonical heptameric fusion motif during bovine coronavirus subgenomic mRNA synthesis. J. Virol. **75:**7362–7374.
34. **Raman, S., P. Bouma, G. D. Williams, and D. A. Brian.** 2003. Stem-loop III in the 5′ untranslated region is a *cis*-acting element in bovine coronavirus defective interfering RNA replication. J. Virol. **77:**6720–6730.
35. **Raman, S., and D. A. Brian.** 2005. Stem-loop IV in the 5′ untranslated region is a *cis*-acting element in bovine coronavirus defective interfering RNA replication. J. Virol. **79:**12434–12446.
36. **Repass, J. F., and S. Makino.** 1998. Importance of the positive-strand RNA secondary structure of a murine coronavirus defective interfering RNA internal replication signal in positive-strand RNA synthesis. J. Virol. **72:**7926–7933.
37. **Sawicki, D., T. Wang, and S. Sawicki.** 2001. The RNA structures engaged in replication and transcription of the A59 strain of mouse hepatitis virus. J. Gen. Virol. **82:**385–396.
38. **Senanayake, S. D., and D. A. Brian.** 1995. Precise large deletions by the PCR-based overlap extension method. Mol. Biotechnol. **4:**13–15.
39. **Sethna, P. B., M. A. Hofmann, and D. A. Brian.** 1991. Minus-strand copies of replicating coronavirus mRNAs contain antileaders. J. Virol. **65:**320–325.
40. **Sethna, P. B., S. L. Hung, and D. A. Brian.** 1989. Coronavirus subgenomic minus-strand RNAs and the potential for mRNA replicons. Proc. Natl. Acad. Sci. USA **86:**5626–5630.
41. **Snijder, E. J., P. J. Bredenbeek, J. C. Dobbe, V. Thiel, J. Ziebuhr, L. L. Poon, Y. Guan, M. Rozanov, W. J. Spaan, and A. E. Gorbalenya.** 2003. Unique and conserved features of genome and proteome of SARS-coronavirus, an early split-off from the coronavirus group 2 lineage. J. Mol. Biol. **331:**991–1004.
42. **Spagnolo, J. F., and B. G. Hogue.** 2000. Host protein interactions with the 3′ end of bovine coronavirus RNA and the requirement of the poly(A) tail for coronavirus defective genome replication. J. Virol. **74:**5053–5065.
43. **Tompkins, W. A., A. M. Watrach, J. D. Schmale, R. M. Schultz, and J. A. Harris.** 1974. Cultural and antigenic properties of newly established cell strains derived from adenocarcinomas of the human colon and rectum. J Natl. Cancer Inst. **52:**1101–1110.
44. **Verheije, M. H., R. C. Olsthoorn, M. V. Kroese, P. J. Rottier, and J. J. Meulenberg.** 2002. Kissing interaction between 3′ noncoding and coding sequences is essential for porcine arterivirus RNA replication. J. Virol. **76:**1521–1526.
45. **Williams, G. D., R. Y. Chang, and D. A. Brian.** 1999. A phylogenetically conserved hairpin-type 3′ untranslated region pseudoknot functions in coronavirus RNA replication. J. Virol. **73:**8349–8355.
46. **Wu, H. Y., J. S. Guy, D. Yoo, R. Vlasak, E. Urbach, and D. A. Brian.** 2003. Common RNA replication signals exist among group 2 coronaviruses: evidence for in vivo recombination between animal and human coronavirus molecules. Virology **315:**174–183.
47. **Yu, W., and J. L. Leibowitz.** 1995. A conserved motif at the 3′ end of mouse hepatitis virus genomic RNA required for host protein binding and viral RNA replication. Virology **214:**128–138.
48. **Yu, W., and J. L. Leibowitz.** 1995. Specific binding of host cellular proteins to multiple sites within the 3′ end of mouse hepatitis virus genomic RNA. J. Virol. **69:**2016–2023.
49. **Zuker, M.** 2003. Mfold web server for nucleic acid folding and hybridization prediction. Nucleic Acids Res. **31:**3406–3415.
50. **Zuniga, S., I. Sola, S. Alonso, and L. Enjuanes.** 2004. Sequence motifs involved in the regulation of discontinuous coronavirus subgenomic RNA synthesis. J. Virol. **78:**980–994.